Chapter 7

Light Sheet Microscopy in Cell Biology

Raju Tomer, Khaled Khairy, and Philipp J. Keller

Abstract

Light sheet-based fluorescence microscopy (LSFM) is emerging as a powerful imaging technique for the life sciences. LSFM provides an exceptionally high imaging speed, high signal-to-noise ratio, low level of photo-bleaching, and good optical penetration depth. This unique combination of capabilities makes light sheet-based microscopes highly suitable for live imaging applications.

Here, we provide an overview of light sheet-based microscopy assays for in vitro and in vivo imaging of biological samples, including cell extracts, soft gels, and large multicellular organisms. We furthermore describe computational tools for basic image processing and data inspection.

Key words: Light sheet microscopy, In vivo imaging, Cell extracts, Quantitative developmental biology, Embryonic development, Image processing

1. Introduction

Noninvasive three-dimensional imaging over time is indispensable for a quantitative understanding of biological processes at multiple scales, from molecular interactions to tissue morphogenesis (1–3). When confocal laser-scanning fluorescence microscopy (CLSM) emerged several decades ago, it provided means for noninvasive three-dimensional imaging of fixed as well as live specimens and, thus, quickly became a standard tool in many laboratories. However, the ever-increasing demand to image for longer periods of time and at higher spatiotemporal resolution is rapidly exposing the limitations of CLSM. The point-scanning implementation of CLSM is inherently slow and causes high levels of photo-bleaching and photo-toxicity, owing to the iterative use of non-selective excitation with high-power beams. Additionally, tissue penetration depth is relatively low. These issues inspired the development of nonlinear microscopy, specifically two-photon microscopy, which provided a substantial increase in the penetration depth and reduction in

Douglas J. Taatjes and Jürgen Roth (eds.), *Cell Imaging Techniques: Methods and Protocols*, Methods in Molecular Biology, vol. 931, DOI 10.1007/978-1-62703-056-4_7, © Springer Science+Business Media, LLC 2013

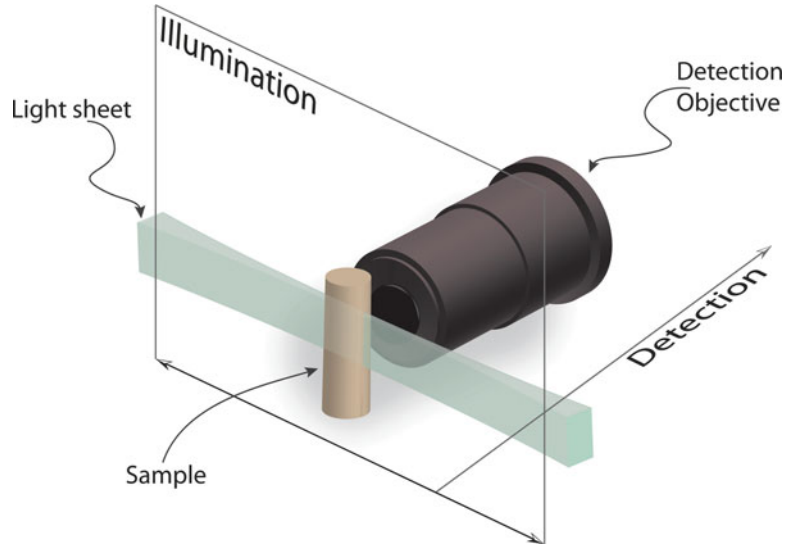

Fig. 1. Light sheet-based microscopy. The central concept in light sheet-based microscopy is to illuminate the specimen in a single plane with a thin sheet of laser light and to record the fluorescence emitted by fluorophores in this thin section with a camera-based detection system oriented at a right angle to the light sheet. The optical sub-systems for illumination and detection are decoupled, which allows using separate objectives optimized for low numerical aperture (NA) specimen illumination and high-NA fluorescence detection. The light sheet is typically generated by scanning a pencil beam through the sample or by focusing a Gaussian beam along one direction into a sheet, using a suitable optical element such as a cylindrical lens.

photo-bleaching, albeit, at the expense of spatial resolution and imaging speed.

In the last decade, Light Sheet Fluorescence Microscopy (LSFM) has emerged to fill the gap resulting from the limitations of CLSM and point-scanning two-photon microscopy. The key concept behind LSFM is sample illumination in a thin volume section from the side and fluorescence detection with an independent optical system at a right angle to the illumination axis (Fig. 1) (4, 5). This is in contrast to confocal microscopy and conventional wide-field microscopy, which typically use the same objective lens for illumination and detection. By illuminating only the in-focus plane, LSFM provides intrinsic optical sectioning and enables simultaneous detection of the fluorescence signal from an entire plane with highly efficient detectors. Thereby, LSFM combines several critical properties, including high acquisition speed, high signal-to-noise ratio, minimal levels of photo-bleaching, and good penetration depth. Moreover, sample preparation typically involves the use of spacious cylindrical compartments formed from thin plastic foils or low-concentration agarose cylinders for sample embedding, which represent a less stressful environment for live biological samples than the traditionally employed glass slide/coverslip (1). LSFM thus combines high-content dynamic imaging with a

more physiological imaging environment and is therefore naturally well-suited for live imaging studies in cell biology and developmental biology (5–7).

Here, we provide an overview of light sheet-based microscopy assays for in vitro and in vivo imaging of biological samples in cell biology and developmental biology. We focus in particular on cell extracts, soft gels, and large multicellular organisms. Since light sheet-based microscopy experiments typically yield large amounts of image data, we also describe computational tools for basic image processing and post-experiment data inspection.

2. Materials

2.1. Sample Preparation in Transparent Plastic Cylinders

1. Transparent plastic foil (bioFOLIE 25, Greiner Bio-One GmbH, see Note 1).

   A different type of plastic foil is also acceptable, as long as it has the following properties: refractive index matched to water (1.33), thickness of less than 50 μm, transparent, and nondisruptive to the imaging process.
2. Glass capillaries (Brand GmbH & Co KG).
3. Hot air welding apparatus (Unitherm K 5.8RS, Zinser Schweisstechnik GmbH).

2.2. Sample Embedding in Soft Agarose Gels

2.2.1. Specimen Embedding

1. Low melting temperature agarose (SeaPlaque Agarose, Lonza).
2. Glass capillaries (2.5 mm outer diameter, 2.0 mm inner diameter, 20 mm length).
3. Heating block (e.g., Thermostat Plus, Eppendorf).
4. Dissection microscope (e.g., SZX7 stereo microscope with SZX2-ILLT-1-5 LED illumination base, Olympus).
5. Petri dishes (e.g., cell culture dish, 100 mm × 20 mm).
6. Pipette and tips.
7. Microscope slides (e.g., SuperFrost Plus, Fisherbrand).
8. High-quality forceps (e.g., Dumont #5).

2.2.2. Drosophila Preparation and Live Imaging

1. *Drosophila* food vials.
2. Apple juice plates.
3. Yeast paste.
4. *Drosophila* mating cages.
5. Sieve.
6. Scalpels.

7. Sodium hypochlorite solution (bleach, Sigma-Aldrich).
8. 0.4% Low melting temperature agarose in tap water (see Subheading 2.2.1).

2.2.3. Zebrafish Preparation and Live Imaging

1. E3 medium:

   For 5 L 60× stock: 87.5 g of 5 mM NaCl, 3.8 g of 0.17 mM KCl, 14.5 g of $CaCl_2 \times 2H_2O$, 24.5 g $MgSO_4 \times 7H_2O$; set pH to 7.2 with NaOH; autoclave.
2. 0.4% Low melting temperature agarose in E3 medium (see Subheading 2.2.1).
3. Pronase (Sigma-Aldrich).

2.3. Light Sheet-Based Microscopy

We use scanned light sheet-based microscopes for live imaging (digital scanned light sheet microscopy, DSLM). Early implementations of fluorescence light sheet microscopy typically relied on stationary mechano-optics to create static laser light sheets for specimen illumination (4, 8, 9). This strategy is still used in many designs and is particularly useful when implementing miniaturized instruments (10, 11) or when performing high-speed 2D imaging, e.g., to record the beating heart in fish embryos (12). Scanned light sheet microscopy (5) introduced a new degree of freedom and enabled the implementation of advanced strategies to light sheet-based specimen illumination. In scanned light sheet microscopy, the specimen is illuminated from the side with a thin pencil beam that is rapidly scanned in one dimension to form a uniform laser light sheet. Using a two-axis scanner, one can furthermore quickly displace the entire light sheet and thereby perform 3D imaging without actually moving the specimen itself. Due to the intrinsic incoherence of the illumination process in scanned light sheet microscopy, light-scattering induced artifacts are greatly reduced if compared to imaging with static light sheets (13, 14). The scanned light sheet microscopy approach forms the basis for high-quality light sheet-based structured illumination (7), high-resolution imaging with "self-healing" Bessel beams (13, 15, 16) and efficient light sheet-based two-photon (2p) excitation (15, 17).

A basic DSLM set-up, such as the instrument described in (5), consists of six sub-systems: (1) a light source, (2) a beam shaping device, (3) a scanning illumination/excitation system, (4) a specimen translating/rotating device, (5) a detection system, and (6) the electronics, electrical devices, computer, and the software. In contrast to standard fluorescence microscopes, e.g., conventional or confocal fluorescence microscopes, which use the same objective lens for excitation and emission detection, the DSLM excitation and fluorescence emission collection systems are operated independently.

The complete DSLM illumination/excitation system (subsystems 1–3 above) consists e.g., of a multi-line argon krypton

laser (e.g., Melles Griot, 35 LTL 835–230), an acousto-optical tunable filter (AOTF; e.g., AA Opto-Electronic, AA.AOTF.nC-400-650nm-PV-TN) for laser wavelength selection and intensity control, a two-axis high-speed scan head (e.g., GSI Lumonics, VM500+), an f-theta lens (e.g., Sill Optics, S4LFT0061/065*), and a low-NA illumination objective lens (e.g., Carl Zeiss, Plan-Apochromat 5x/0.16) operated with a regular tube lens. The illumination/excitation objective lens is mounted on a piezo nanofocus (e.g., Physik Instrumente, P-725.CLQ), which can move the lens 400 μm along its optical axis. The specimen is placed inside a custom specimen chamber made e.g., from inert black Delrin. The specimen chamber features a temperature control system, which includes a temperature sensor inside the chamber and a heating foil attached below the chamber.

Typically, long-working distance water-dipping objectives are used in the DSLM detection system (e.g., Carl Zeiss: Plan-Neofluar 2.5x/0.075, Fluar 5x/0.25, C-Apochromat 10x/0.45 W, Plan-Apochromat 20x/1.0 W, or Plan-Apochromat 63x/1.0 W) and mounted on a second independently operated piezo nanofocus. The detected light is filtered by long-pass filters (e.g., Semrock RazorEdge RU 488 LP, RU 568 LP, or RU 647 LP) mounted on a filter wheel (e.g., Ludl, 96A354), passes through a tube lens (e.g., Carl Zeiss, 164.5 mm focal length), and is recorded with a CCD camera (e.g., PCO AG, pco.2000).

The illumination and detection sub-systems are complemented by a specimen positioning system, which consists of a set of three linear translation stages (e.g., Physik Instrumente, M-111K028) and one micro-rotary stage (e.g., Physik Instrumente, M-116.DG). The rotary stage with its customized port provides connectors for anodized aluminum specimen holders that hold glass capillaries and plastic syringes.

The DSLM's acquisition computer comprises a multi-core CPU (e.g., Intel Core 2 Quad Q6600, 2.4 GHz) and a high-performance hardware RAID controller (e.g., Promise, SuperTrak EX8350) with a multi-Terabyte RAID-0 disk array. Data transfer for up to two cameras is facilitated via a dual-camera-link controller card (e.g., National Instruments, PCIe-1430), which is installed in the acquisition computer as well. The other electronics controller cards are located in the DSLM electronics hub, which is attached to the computer via an Ethernet-linked bus extender (e.g., Hartmann Elektronik, StarFabric Bridge). The electronics hub includes the scan controller (e.g., GSI Lumonics, HC/3), a four-channel stage controller (e.g., Physik Instrumente, C-843.41), two multi-channel I/O controllers (e.g., National Instruments, PCI-6733), and the custom mainframe relay system. The AOTF beam control unit (e.g., AA Opto-Electronic, AA.MOD.8C-C**-75.158.24VDC) with an independent linear power supply (e.g., Kniel, CA 24.2,5), the dual-channel scanner drivers (e.g., GSI Lumonics, MiniSax) with dedicated linear power supplies (e.g., Kniel,

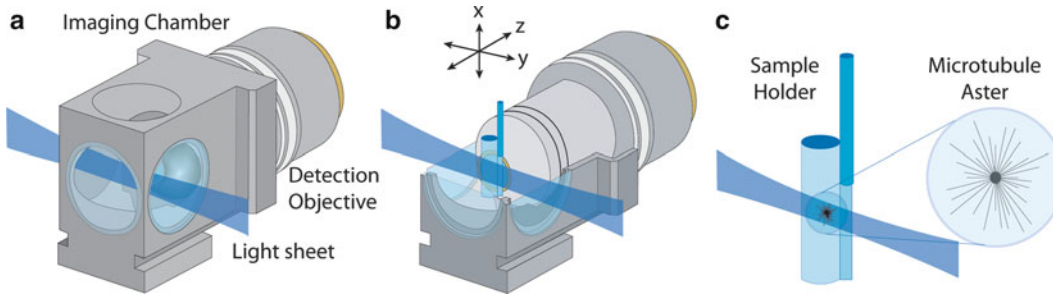

Fig. 2. Light sheet-based imaging of microtubule asters in egg extracts using transparent plastic cylinders. (**a**) Illustration (to scale) of the light sheet imaging arrangement. The detection lens in the central imaging chamber is immersed in water. The light sheet is focused into the chamber from the side and illuminates a thin volume section of the specimen. (**b**) The sample cylinder containing the egg extract is attached to a glass capillary and oriented parallel to gravity. The cylinder is located in front of the detection lens and can be moved along three dimensions via a set of linear miniature stages. The detector elements, including the microscope objective lens, are oriented at a right angle to the light sheet. The focal plane of the detection lens is coplanar with the light sheet. (**c**) The microtubule asters are polymerized in the egg extract inside the plastic cylinder. The cylinder has a diameter of approximately 2 mm and consists of a thin plastic foil with a thickness of 25 μm, which is gas-permeable but water-impermeable. The membrane has a high light transmittance at visible wavelengths and its refractive index is matched to the water in the imaging chamber. Due to the high viscosity of the egg extract, the polymerized asters can be kept in a stable position anywhere inside the sample cylinder. The distance between the cylinder's surface and the recorded asters is typically on the order of 100 μm. Three-dimensional image data are recorded by moving the microtubule asters in small steps through the light sheet while simultaneously recording images with the CCD camera. Credits: Reprinted from *Biophysical Journal*, vol. 95, Keller et al., "Three-Dimensional Microtubule Behavior in *Xenopus* Egg Extracts Reveals Four Dynamic States and State-Dependent Elastic Properties," 1474–1486, Copyright (2008), with permission from Elsevier.

CA 15.4) and the custom environmental control system for the specimen chamber are in a separate housing.

The DSLM control software of our instrument described in (5) was developed in .NET framework 3.0 (Microsoft), using the programming language C# for user interface and high-level control layers and C++ for lower-level hardware communication.

2.4. Basic Image Processing

1. ImageJ (http://rsb.info.nih.gov/ij/) or Fiji (http://fiji.sc/wiki/index.php/Fiji).
2. Matlab (The Mathworks Incorporated, http://www.mathworks.com).

3. Methods

Light sheet-based microscopes often rely on long-working distance water-dipping objectives for fluorescence detection and, therefore, require sample immersion in an aqueous fluid (Fig. 2). Moreover, if specimens are subjected to multi-view imaging, they must be optically accessible for light sheet illumination and fluorescence detection from multiple angles (18). These two requirements often

introduce challenges in the sample preparation. We developed protocols for live imaging of cell extracts, soft gels, and entire embryos embedded in agarose gels that fulfill these requirements and allow time-lapse data acquisition in a physiologically relevant context over long periods of time.

3.1. Sample Preparation Protocol for In Vitro Imaging of Cell Extracts and Soft Gels

We developed a three-dimensional sample preparation technique in transparent plastic polymer cylinders for the observation of live specimens embedded in soft gels as well as the imaging of cytoskeletal filament dynamics in *Xenopus laevis* egg extracts (6, 19). Since these samples should not be directly exposed to the aqueous medium in the imaging chamber of the light sheet-based microscope, we are using thin plastic foils to create transparent isolated sample compartments. These plastic chambers were tested extensively in the context of live imaging of microtubule dynamic instability in small volumes of *X. laevis* egg extracts (10–20 μL). The light sheet can easily enter these chambers from any side, with the exception of a small angular range that is inaccessible due to a welding seam resulting from the production process (see Fig. 3).

3.1.1. Preparing Cell Extracts and Soft Gels in Plastic Cylinders

1. Place a glass capillary in the middle of a rectangular piece of plastic foil with a size of about 50 mm × 100 mm, such that the capillary is oriented parallel to the long edges of the plastic foil. The capillary functions as a template for the cylindrical plastic chamber. Note that one side of the plastic foil is hydrophobic, whereas the other side is hydrophilic. Make sure that the glass capillary is placed on the hydrophilic side of the foil, such that this side will be the inner surface of the plastic cylinder.
2. Turn the foil over at one of the long edges, such that the foil encloses the glass capillary.
3. Use the hot air welding apparatus to form the seam of a plastic cylinder along the side of the glass capillary. Upon welding, the glass capillary can be removed.
4. Cut the approximately 100 mm long plastic cylinder into shorter pieces with a length of about 15 mm each.
5. Seal one end of each of these small cylinders by using the hot air welding apparatus.
6. Remove extra plastic foil at the two seams of each plastic cylinder with a pair of scissors.
7. Reinforce the welding seams by carefully dipping the plastic foil at each seam into clear silicone glue.
8. Glue the long seam of each plastic cylinder to a glass capillary. A photograph of a complete plastic cylinder including glass capillary is shown in Fig. 3.
9. Allow the glue to solidify for about 1 day before using the plastic cylinder in an imaging experiment.

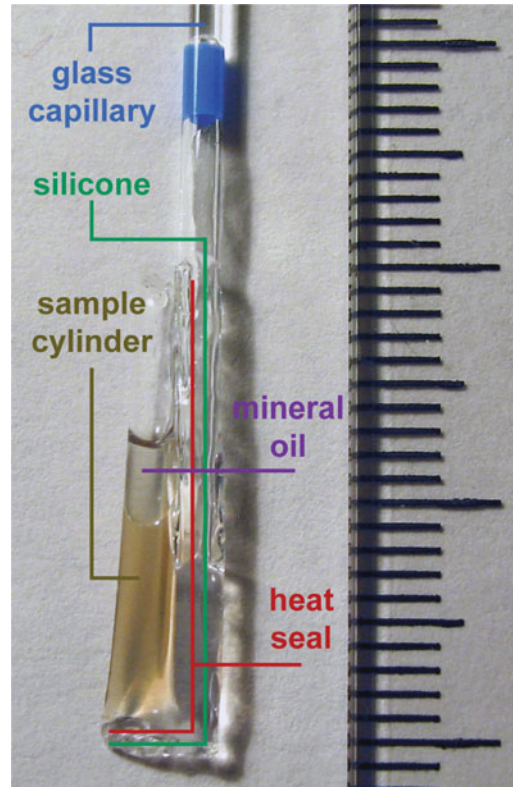

Fig. 3. Sample preparation of egg extracts in transparent plastic cylinders. The photo shows a polytetrafluorethylen (PTFE) cylinder loaded with *Xenopus laevis* egg extract. The cylinder is formed using a 25-μm-thin transparent plastic foil. The *bottom* part and lateral part of the plastic cylinder are sealed by welding using hot air. The seams are reinforced by transparent silicone glue. The heat seals prevent contact of the silicone glue with the specimen inside the plastic cylinder. A glass capillary is glued to the cylinder with transparent silicone glue and acts as a sample holder in the light sheet microscope. A layer of mineral oil is added on *top* of the egg extract to prevent degradation by exposure to air. Scale: major tick mark spacing = 10 mm, minor tick mark spacing = 1 mm.

10. Prepare the egg extract or specimen in a soft gel mix and transfer it to the plastic cylinder using a laboratory pipette.
11. Add a thin layer of mineral oil on top of the egg extract or soft gel in order to prevent air contact and to reduce the rate of dehydration/degradation.

3.2. Sample Preparation Protocol for In Vivo Imaging of Drosophila and Zebrafish Embryos

3.2.1. Embedding Drosophila Embryos (See Note 2)

1. Set up transgenic flies of interest in a cage with a grape juice plate at the bottom, ideally on the evening before the imaging experiment. On the next morning, replace the old plate with a fresh one containing a drop of yeast paste in the center, which acts as a stimulant of fly mating behavior. This ensures that the batch of fresh embryos is reasonably well synchronized.
2. Collect embryos by removing the plate from the cage. The embryonic chorion (eggshell) is optically less clear and therefore

significantly affects image quality. It can be removed using common bleach, without compromising the viability of the embryos. For this purpose, first remove the yeast paste by carefully cutting out the piece of grape juice food substrate using a scalpel. Next, fill the plate with 50% bleach/H_2O and leave it for appoximately 1 min with occasional shaking. The majority of embryos should start to float. Pour the embryos through a fine sieve, followed by several washes with tap water. Finally, collect the embryos in an agarose-coated Petri dish. An agarose coating of a few millimeters thickness is sufficient.

3. Select transgenic embryos of appropriate age under a dissection and fluorescence microscope. Use one arm of a forceps to lift the embryo from below. The embryo will stick at the tip of the forceps. Next, fill a 2.5 mm capillary with 0.4% melted agarose/H_2O (kept at 30 °C in a heating block) by dipping in a 1.5 mL Eppendorf tube. Since the agarose will start to solidify within about 20–30 s, the embryo has to be embedded quickly.
4. Place the capillary under a dissection microscope and put the embryo inside the agarose by inserting one arm of the forceps (with the embryo at the tip) into the capillary in a single quick move (preventing the embryo from being trapped at the agarose surface due to the high surface tension). The embryo should usually detach from the forceps tip. If not, gently tap the backside of the forceps on the capillary wall. The embryo can be oriented by moving the forceps tip around it, such that a flow is introduced in the surrounding agarose.
5. Store the embedded samples in tap water and proceed with imaging.

3.2.2. Embedding Zebrafish Embryos (See Note 2)

1. Set up fish mating tanks in the night. Remove tank dividers in the morning, and collect early stage embryos within an hour. Perform embryonic micro-injections, if needed.
2. Dechorionate embryos either manually or enzymatically. In brief, use a pair of forceps to hold the chorion with one forceps and tear open the chorion with the other forceps. Next, hold the chorion in a location opposite of the initial incision and gently push the embryo through the opening. Younger embryos are particularly fragile and require great care to avoid damage. Alternatively, an enzymatic treatment (Pronase) can be used to efficiently dechorionate larger amounts of eggs.
3. The dechorionated embryos are very sensitive to any manipulation. To minimize damage, use a glass capillary fitted in a pipette tip (by cutting the pipette tip's end such that the capillary fits tightly, see Note 3) to transfer and embed embryos. First, transfer the embryo together with some medium to a microscope glass slide. Remove any excess medium, but leave enough to avoid air exposure. Gently pour a drop of 0.4%

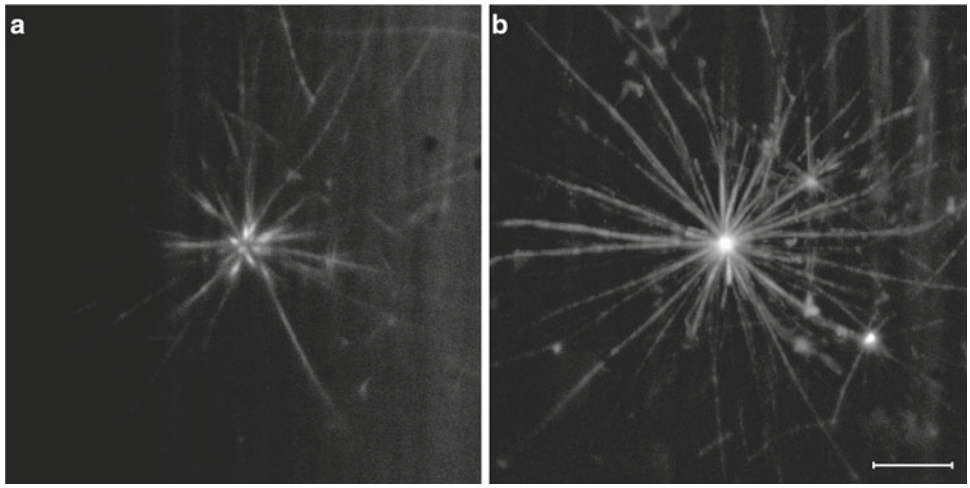

Fig. 4. Light sheet-based imaging of a microtubule aster in *X. laevis* egg extract. (**a**) Single frame of the three-dimensional image stack. (**b**) Maximum-intensity projection of the three-dimensional image stack, which contains 68 planes at a 300 nm z-spacing. Microtubules oriented in parallel to the plane of observation appear dimmer than microtubules in a perpendicular orientation. Tubulin was labeled with TAMRA. Objective: Carl Zeiss Achroplan 100x/1.0 W. Scale: 10 μm. Credits: Reprinted from *Current Opinion in Cell Biology*, vol. 18, Keller et al., "Life Sciences Require the Third Dimension," 117–124, Copyright (2006), with permission from Elsevier.

agarose/H_2O (kept at 30 °C in a heating block) onto the embryo. Use the agarose-coated (by briefly dipping in agarose) glass capillary to gently pull up the embryo along with agarose. This should be performed under the dissecting microscope to avoid damaging the embryo. Note that it is generally difficult to orient the embryo using tools. Instead, simply push the embryo out and pull it in again until it comes to rest in the preferred orientation.

4. Store the embedded samples in E3 medium and proceed with imaging.

3.3. Light Sheet-Based Microscopy Imaging Protocol

Considering that, at the time of this writing, light sheet-based microscopes are non-commercial custom instruments, the precise steps in this section depend substantially on the specific implementation of the instrument. We will therefore only outline the basic procedure assuming a DSLM-like instrument, comparable to the microscope described in section 2.3 (see also (20)).

1. Carefully insert sample holder into the port of the rotary stage. Make sure that only a minimal amount of force is applied when locking the holder in the stage's port. Try to support the rotary stage with the other hand when inserting and locking the holder.
2. Option 1 (imaging specimens in cell extracts and soft gels using plastic cylinders, Fig. 4): Move the plastic cylinder with the extract/gel in front of the detection objective's lens (by moving the respective linear stage). Option 2 (imaging embryos in

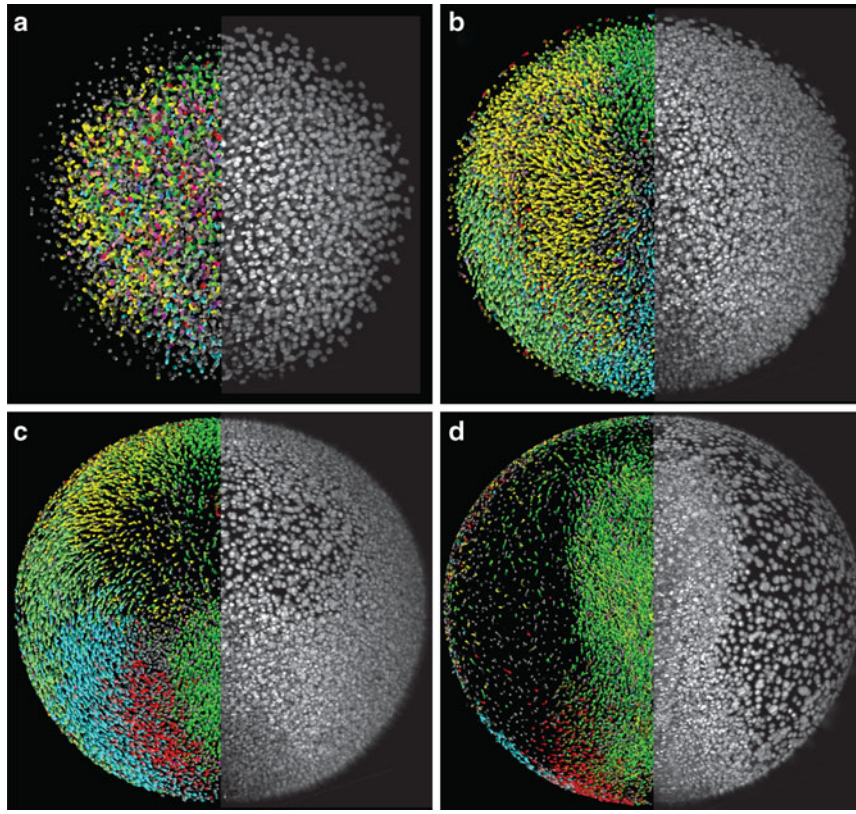

Fig. 5. Global cell tracking in zebrafish embryos with scanned light sheet microscopy. DSLM microscopy data (*right half* of embryo: animal view, maximum-intensity projection) and the subsequently reconstructed "digital embryo" (*left half* of embryo) with color-encoded cell migration directions. Time points: 289 minutes post fertilization (mpf) (**a**), 368 mpf (**b**), 599 mpf (**c**), 841 mpf (**d**). Color code: dorsal migration (*cyan*), ventral migration (*green*), toward or away from body axis (*red* or *yellow*), toward yolk (*pink*). Objective: Carl Zeiss C-Apochromat 10x/0.45 W. Databases and high-resolution movies of the digital zebrafish embryo are available at http://www.digital-embryo.org. Credits: Reprinted from *Science*, vol. 322, Keller et al., "Reconstruction of Zebrafish Early Embryonic Development by Scanned Light Sheet Microscopy," 1065–1069, Copyright (2008), with permission from AAAS.

agarose cylinders, Fig. 5): Move the end of the glass capillary with the specimen just above the detection objective's lens (by moving the respective linear stage). If you are using an upright specimen positioning system, move the end of the glass capillary just below the detection objective's lens. Carefully push the agarose cylinder out of the glass capillary, such that the specimen is located directly in front of the detection lens.

3. Point a cold light source at the sample chamber and activate the camera in order to locate the specimen. Use the linear and rotary stages to identify the volume of interest.
4. Deactivate the cold light source and switch to fluorescence mode (activate laser and laser scanner, enable fluorescence detection filter) in order to determine the optimal acquisition parameters, including exposure time, laser power, and z-range of the image stack. To achieve good z-sampling, the z-step size

(spatial interval between images in the z-stack) should be set to 50–70% of the central light sheet thickness.

5. Define the experiment parameters (considering options such as z-stack settings, time-lapse parameters, multi-view settings) and start image acquisition.

3.4. Basic Image Processing and Data Inspection in Light Sheet-Based Microscopy

The main data processing challenges the LSFM microscopist is facing routinely are as follows:

- Large data sets in three and four dimensions must be stored and managed.
- Images need to be deconvolved.
- Image registration and fusion is necessary for multiview image reconstruction.

We typically use ImageJ (http://rsb.info.nih.gov/ij/) or Fiji (http://fiji.sc/wiki/index.php/Fiji), as well as Matlab (The Mathworks Inc., http://www.mathworks.com) as the main tools for LSFM image processing.

3.4.1. Deconvolution

The Lucy-Richardson (LR) method (21) has been successfully used for the deconvolution of LSFM images (5, 7). The main steps are given below:

1. Three-dimensional image volumes are imported into Matlab by sequentially reading individual two-dimensional frames from disk with the command *imread*. This constructs a three-dimensional matrix representation in Matlab.
2. A PSF is defined. The PSF can either be experimentally determined by imaging a sub-pixel-sized fluorescent bead or theoretically calculated based on the imaging conditions. This PSF is also imported into (or calculated in) Matlab and represented as a three-dimensional matrix.
3. The built-in LR filter is executed using the command *deconvlucy* (see Note 4).

3.4.2. Image Registration and Fusion

Multiview imaging yields images that are spatially complementary and partially overlapping. By fusing these images, we eliminate anisotropy and produce a single enhanced image with better resolution and improved uniformity of image quality. This is especially important in the case of optically dense samples and comprises one of the major advantages of using LSFM.

At the time of this writing, there are two main methods for LSFM data fusion. The first one (18) takes advantage of frequency information in the images, and performs simultaneous fusion and deconvolution. The steps involved in this process are:

1. Preprocessing of each view: This involves rescaling the axial dimension to obtain an isotropic dataset, followed by rotation

to a reference frame, for example the orientation of the first view. Both steps can be accomplished by using bicubic interpolation either in ImageJ or Matlab.

2. Registration of all views (see Note 5): The above transformation is generally insufficient, and must be fine-tuned to maximize the overlap of all views. To register the views, only translation is considered, whose vectors are determined by cross-correlation, implemented using the fast Fourier transform. Registration depends on some minimal amount of overlap between the images. Since for some view pairs this overlap is not sufficient, this registration depends on a "running sum" approach. Adjacent views (which typically share the most overlap) are registered as a pair first. Their sum is then used as a registration target for the next adjacent view. After one round of this process, the views are fused by taking the weighted average of the registered views in Fourier space. The weights are given by the expected signal-to-noise ratio. This fused image is used, in a second stage, as the target for another round of registration. The process iterates until the registration corrections are less than a pixel.
3. Fusion combined with deconvolution (see Note 5): The registered images are convolved with the PSF (either experimentally determined or theoretically calculated, and normalized to integrate to unity), to produce a set of simulated images. Based on this set, correction coefficients are calculated using a regularized inverse filter. These coefficients are fused with the weighted average described above, and added to the estimate from the previous iteration to yield an updated estimate. The sample distribution is constrained to be non-negative and normalized, and is then compared to the previous one. If the change due to the update is sufficiently small, the fusion is complete; otherwise another iteration of deconvolution is performed. The regularization parameter needed in the inverse filtering step is optimized manually on a small region of the image.

The second method, due to Preibisch et al. (22), requires fluorescent beads acting as fiducials to be present in the agarose gel. The main idea is that the bead locations are determined in a first step, and then the transformation that maximizes the overlap of all local bead constellations (point clouds) is estimated. This transformation is then applied to the original images. The method provides a fast and robust registration. Content-based fusion, combined with nonlinear blending gives the final fusion result. The code is made available through a Fiji plugin (http://pacific.mpi-cbg.de/wiki/index.php/SPIM_Registration).

4. Notes

1. The decision of using the 25-μm-thin bioFOLIE 25 instead of a thicker foil, such as the 50-μm-thin bioFOLIE 50, was based on an investigation of its optical properties and amenability for light microscopy assays. Light sheet-based microscopy recordings of small fluorescent beads in distilled water inside plastic cylinders constructed from both types of foils showed that the imaging quality inside the bioFOLIE 25 cylinders is only slightly affected by the foil, whereas the bioFOLIE 50 introduces significant optical aberrations and is clearly less well-suited for biological imaging assays.
2. Embryos require great care to avoid damage. For specimen orientation, use forceps to move the agarose around the embryo. Also, embryos can get stuck at the surface of the liquid agarose. In such cases, discard the sample and start with a fresh one.
3. We typically use a glass capillary coated with agarose to transfer the specimens from the Petri dish to a microscopic slide. The agarose coating is applied by briefly dipping the capillary in liquid agarose.
4. The quality of the output image is sensitive to the accuracy of the PSF and to the number of LR iterations. Too few iterations would not provide a good reconstruction, too many introduce speckle artifacts. We found ten iterations to give good results for most experiments. The optimal number depends on the image signal-to-noise ratio. This has been taken into account in a program called AIDA (23), which determines the optimal convergence automatically. Moreover, in the absence of an accurate PSF, the CPU-expensive blind deconvolution strategy can be used (Matlab command *deconvblind*). In cases where the input images are too large to be held in memory at once, they can be divided into overlapping "slabs" and stitched together after deconvolution.
5. The registration and fusion are implemented in Matlab with the exception of the computation-intensive Fast Fourier Transform, which was implemented in Visual C# .NET (Microscoft Corporation). Further performance improvements are achieved by utilizing Intel Integrated Performance Primitives (Intel Corporation). The code can fuse time-lapse series of whole embryos over the course of a few days on a conventional desktop PC. For code availability see the original publication.

Acknowledgement

This work was supported by the Howard Hughes Medical Institute.

References

1. Keller PJ, Pampaloni F, Stelzer EHK (2006) Life sciences require the third dimension. Curr Opin Cell Biol 18:117–124
2. Keller PJ, Stelzer EH (2008) Quantitative in vivo imaging of entire embryos with digital scanned laser light sheet fluorescence microscopy. Curr Opin Neurobiol 18:624–632
3. Khairy K, Keller PJ (2011) Reconstructing embryonic development. Genesis 49(7): 488–513
4. Huisken J, Swoger J, Del Bene F, Wittbrodt J, Stelzer EHK (2004) Optical sectioning deep inside live embryos by selective plane illumination microscopy. Science 305:1007–1009
5. Keller PJ, Schmidt AD, Wittbrodt J, Stelzer EHK (2008) Reconstruction of zebrafish early embryonic development by scanned light sheet microscopy. Science 322:1065–1069
6. Keller PJ, Pampaloni F, Stelzer EH (2007) Three-dimensional preparation and imaging reveal intrinsic microtubule properties. Nat Methods 4:843–846
7. Keller PJ, Schmidt AD, Santella A, Khairy K, Bao Z, Wittbrodt J, Stelzer EH (2010) Fast, high-contrast imaging of animal development with scanned light sheet-based structured-illumination microscopy. Nat Methods 7:637–642
8. Fuchs E, Jaffe J, Long R, Azam F (2002) Thin laser light sheet microscope for microbial oceanography. Opt Express 10:145–154
9. Voie AH, Burns DH, Spelman FA (1993) Orthogonal-plane fluorescence optical sectioning: three-dimensional imaging of macroscopic biological specimens. J Microsc 170:229–236
10. Engelbrecht CJ, Voigt F, Helmchen F (2010) Miniaturized selective plane illumination microscopy for high-contrast in vivo fluorescence imaging. Opt Lett 35:1413–1415
11. Turaga D, Holy TE (2008) Miniaturization and defocus correction for objective-coupled planar illumination microscopy. Opt Lett 33:2302–2304
12. Scherz PJ, Huisken J, Sahai-Hernandez P, Stainier DY (2008) High-speed imaging of developing heart valves reveals interplay of morphogenesis and function. Development 135:1179–1187
13. Fahrbach FO, Simon P, Rohrbach A (2010) Microscopy with self-reconstructing beams. Nat Photonics 4:780–785
14. Rohrbach A (2009) Artifacts resulting from imaging in scattering media: a theoretical prediction. Opt Lett 34:3041–3043
15. Planchon TA, Gao L, Milkie DE, Davidson MW, Galbraith JA, Galbraith CG, Betzig E (2011) Rapid three-dimensional isotropic imaging of living cells using Bessel beam plane illumination. Nat Methods 8:417–423
16. Fahrbach FO, Rohrbach A (2010) A line scanned light-sheet microscope with phase shaped self-reconstructing beams. Opt Express 18:24229–24244
17. Truong TV, Supatto W, Koos DS, Choi JM, Fraser SE (2011) Deep and fast live imaging with two-photon scanned light-sheet microscopy. Nat Methods 8(9):757–760
18. Swoger J, Verveer P, Greger K, Huisken J, Stelzer EH (2007) Multi-view image fusion improves resolution in three-dimensional microscopy. Opt Express 15:8029–8042
19. Keller PJ, Pampaloni F, Lattanzi G, Stelzer EHK (2008) Three-dimensional microtubule behavior in Xenopus egg extracts reveals four dynamic states and state-dependent elastic properties. Biophys J 95:1474–1486
20. Keller PJ, Stelzer EH (2010) Digital scanned laser light sheet fluorescence microscopy. Cold Spring Harb Protoc 2010:pdb.top78
21. Lucy LB (1974) An iterative technique for the rectification of observed distributions. Astron J 79:745–754
22. Preibisch S, Saalfeld S, Schindelin J, Tomancak P (2010) Software for bead-based registration of selective plane illumination microscopy data. Nat Methods 7:418–419
23. Hom EFY, Marchis F, Lee TK, Haase S, Agard DA, Sedat JW (2007) AIDA: an adaptive image deconvolution algorithm with application to multi-frame and three-dimensional data. J Opt Soc Am A 24:1580–1600